Neuropharmacology 158 (2019) 107748

Contents lists available at ScienceDirect

Neuropharmacology

journal homepage: www.elsevier.com/locate/neuropharm

The diabetes drug semaglutide reduces infarct size, inflammation, and apoptosis, and normalizes neurogenesis in a rat model of stroke

Xiaoyan Yang[a], Peng Feng[a,*], Xiangjian Zhang[b,c], Dongfang Li[a], Ruifang Wang[a], Chenhui Ji[e], Guanglai Li[a], Christian Hölscher[d]

[a] Department of Neurology, The Second Affiliated Hospital of Shanxi Medical University, No. 382 Wuyi Road, Taiyuan, 030001, Shanxi Province, China
[b] Department of Neurology, Second Hospital of Hebei Medical University, Shijiazhuang, 050000, China
[c] Hebei Collaborative Innovation Center for Cardio-Cerebrovascular Disease, Shijiazhuang, 050000, China
[d] Research and Experimental Center, Henan University of Chinese Medicine, 156 Jinshui Dong Road, Zhengzhou, 450000, Henan province, China
[e] Center for Translational Neurodegeneration and Regenerative Therapy, Shanghai Tenth People's Hospital Affiliated to Tongji University School of Medicine, Shanghai, 200072, China

HIGHLIGHTS

- Semaglutide is a new diabetes drug on the market.
- Semaglutide has neuroprotective properties in a stroke animal model.
- Motor activity was improved and infarct volume reduced by the drug.
- Loss of neurons and inflammation was reduced.
- Neurogenesis and growth factor cell signaling was normalized.

ARTICLE INFO

Keywords:
Stroke
Growth factor
GLP-1
Rat
PMCAO
Ischemia

ABSTRACT

Stroke is a condition with few medical treatments available. Semaglutide, a novel Glucagon-like peptide-1 (GLP-1) analogue, has been brought to the market as a treatment for diabetes. We tested the protective effects of semaglutide against middle cerebral artery occlusion injury in rats. Animals were treated with 10 nmol/kg bw ip. starting 2 h after surgery and every second day for either 1, 7, 14 or 21 days. Semaglutide-treated animals showed significantly reduced scores of neurological impairments in several motor and grip strength tasks. The cerebral infarction size was also reduced, and the loss of neurons in the hippocampal areas CA1, CA3 and the dentate gyrus was much reduced. Chronic inflammation as seen in levels of activated microglia and in the activity of the p38 MAPK – MKK – c-Jun- NF-κB p65 inflammation signaling pathway was reduced. In addition, improved growth factor signaling as shown in levels of activated ERK1 and IRS-1, and a reduction in the apoptosis signaling pathway C-raf, ERK2, Bcl-2/BAX and Caspase-3 was observed. Neurogenesis had also been normalized by the drug treatment as seen in increased neurogenesis (DCX-positive cells) in the dentate gyrus and a normalization of biomarkers for neurogenesis. In conclusion, semaglutide is a promising candidate for re-purposing as a stroke treatment.

1. Introduction

Ischemic stroke is one of the leading causes of death and adult disability world wide. Stroke is often associated with co-morbid conditions such as diabetes that increase the risk and severity of stroke (Marini et al., 2004){Marini et al., 2004 #5855;Wang et al., 2019 #44}. Inflammation and apoptosis play an important role in cerebral ischemic pathogenesis and may represent a target for treatment (Wang et al., 2019). This process can be reduced or blocked by cell survival and growth factor signaling. Glucagon-like peptide 1 (GLP-1) is a growth factor and peptide hormone which has neuroprotective effects in a range of animal models of disease such as Alzheimer's disease, Parkinson's disease, and stroke (Han et al., 2016; Holscher, 2014a, 2018; Li et al., 2009). The GLP-1 receptor is expressed by neurons in the brain,

* Corresponding author.
E-mail address: juven15@163.com (P. Feng).

https://doi.org/10.1016/j.neuropharm.2019.107748
Received 9 June 2019; Received in revised form 18 August 2019; Accepted 22 August 2019
Available online 26 August 2019

and the peptide is transported across the blood-brain barrier (Darsalia et al., 2012; Hamilton and Holscher, 2009; Kastin et al., 2002; Lee et al., 2011; Teramoto et al., 2011).

Protease-resistant GLP-1 receptor agonists with a longer survival time in the blood have been developed as treatments for diabetes (Christensen et al., 2011; Lovshin and Drucker, 2009). Several studies have shown good neuroprotective effects of the GLP-1 receptor agonist exendin-4 in animal models of ischemic stroke (Darsalia et al., 2014; Lee et al., 2011). DPP-IV inhibitors that extend the half-life of GLP-1 in the blood also showed protective effects in stroke models (Darsalia et al., 2016). The newer GLP-1 analogue liraglutide that has a longer biological half-life in the blood stream was protective in different ischemic reperfusion and stroke animal models, too (Briyal et al., 2014; Sato et al., 2013). Liraglutide has shown good neuroprotective effects in animal models of Alzheimer's disease (McClean and Holscher, 2014) and also in Parkinson's disease (Liu et al., 2015). The drug also showed protective effects in the middle cerebral artery occlusion (MCAO) animal model (Briyal et al., 2014; Sharma et al., 2014). Liraglutide pretreatment resulted in a smaller infarct size as well as fewer neurological and motor function deficits (Briyal et al., 2014; Sharma et al., 2014). Liraglutide (Victoza) has been prescribed as a treatment for type II diabetes for many years with good outcomes and few side effects (Ahren, 2014; Marso et al., 2016b).

Semaglutide is a modification of liraglutide that is protease-resistant by changing the amino acid at position 8 and an extended spacer for the attached fatty acid which extends the survival time of the peptide in the blood (Lau et al., 2015). It has been approved in the USA and Europe as a once-weekly treatment for diabetes (Dhillon, 2018; Hedrington et al., 2018). A phase II clinical trial testing semaglutide in patients with Parkinson's disease will start in 2019 (NCT03659682). Semaglutide is effective in treating diabetes and additionally improves cardiovascular outcomes in patients (Marso et al., 2016a).

The permanent middle cerebral artery occlusion (pMCAO) model in the rat has been an invaluable tool for the study of permanent and transient focal cerebral ischemia, and is one of the most widely used focal cerebral ischemia models (Bardutzky et al., 2005). The pMCAO model was used over the transient MCAO, due to the avoidance of reperfusion injury in our research model aimed at providing new insight into the semaglutide neuroprotective effects in the rat brain. We therefore set out to test semaglutide in this model to evaluate its potential as a treatment for stroke. Our previous research showed good protective effects of semaglutide in a mouse model of Parkinson's disease, and we used the same dose in this study (Zhang et al., 2018, 2019). We analyzed key pathological processes such as infarct volume and neuronal death in the hippocampus, motor impairments, chronic inflammation, apoptosis, and neurogenesis. Hippocampal neurogenesis in the granule cell layer (GCL) of the dentate gyrus (DG) takes place throughout life span in virtually all mammals including humans via division of neural stem/progenitor cells (NSCs) located in the subgranular zone (SGZ) of the DG (Gould et al., 1997; Kempermann et al., 2015; Kuhn et al., 1996). Neurogenesis has the potential to reduce neuronal damage by replacing lost neurons (Greenberg and Jin, 2006; Zhang et al., 2008). We furthermore analyzed growth factor cell signaling to assess if impaired neurogenesis neuroblasts proliferation and cell growth and repair can be restored by semaglutide.

2. Materials and methods

2.1. Animals

Adult male Sprague–Dawley (SD) rats weighing 250–300 g aged three months were obtained from the Academy of Military Medical Sciences (AMMS China). All animal procedures were licensed by the Shanxi Medical University ethics committee and performed in accordance to National Institute of Health (NIH) guideline and the ARRIVE guidelines (Animal Research: Reporting in Vivo Experiments). Animals were caged in a cage of two to three and maintained on a 12 h/12 h light/dark cycle, in temperature-controlled room (T:22 °C ± 2). Food and water were available ad libitum. For rats used for cerebral ischemia experiments, there was a 7-day acclimation period prior to experiments.

2.2. Experimental groups and drug administration

Semaglutide (MW = 3765, with purity of 97% was dissolved in 0.9% NaCl) was obtained from Chinapeptides Ltd (Shanghai, China). Purity and quality was tested by HPLC and Mass-Spec techniques.

The amino acid sequence of semaglutide (Lau et al., 2015): HXEGTFTSDVSSYLEGQAAKN6-(*N*-(17-carboxy-1-oxoheptadecyl)-L-gamma-glutamyl-2-(2-(2-aminoethoxy)ethoxy)acetyl-2-(2-(2-aminoethoxy)ethoxy)acetyl)EFIAWLVRGRG-OH

X = aminoisobutyric acid;

144 138 Male Sprague-Dawley rats were randomly divided into three groups as follows (n = 48 46 in each group):Group 1: rats as the sham operated group that received equal volume saline (Sham); group 2: vehicle controls that received equal volume saline (Vehicle); group 3: semaglutide rats that received semaglutide at 10 nmol/kg (Semaglutide). Each group was further divided into subgroups of four time-points (1d,7d,14d,21d). At 2 h after MCAO, rats in the semaglutide group were injected with semaglutide intraperitoneally (10 nmol/kg), in the case of vehicle and sham operated group, equal volume saline was administered in the same manner, then continuously injected every second day for 1, 7, 14 and 21 days. Added content:10 rats were randomly taken from each group for observation of blood glucose, body weight and behavior tests. Blood glucose, body weight and behavioral indexes were measured at each time point (1d, 7d, 14d,21d), the rats were observed for 21 days and then sacrificed for tissue sampling. At the indicated time points, rats were sacrificed by decapitation under deep anesthesia and their brains were removed for Immunohistochemical analysis (12 rats in each group, 3 rats at each time point), Immunofluorescence (12 rats in each group, 3 rats at each time point) and Western blot experiments (12 rats in each group, 3 rats at each time point). If some rats died after pMCAO, we repeated the experiment with a fresh batch of rats to ensure that at least 10 rats in each group were observed for 21 days to measure blood glucose, body weight and behavioral indicators, and at each time point at least 3 rats were studied for Immunohistochemical, Immunofluorescence and Western blot experiments, respectively. All experiments were conducted by a person blinded to treatments.

2.3. Measurement of blood glucose

Blood was aseptically collected from the tail vein of the animals 1 day before MCAO, during the process of surgery, and 1, 7, 14 and 21days after MCAO under halothane anesthesia. A drop of blood was collected from the animal's tail and used for measuring the blood glucose level using a portable glucose meter (Sinocare Inc, China) according to the manufacturer's instructions. Levels were reported as mmol/l.

2.4. Body weight measurements

Body weight was assessed using a small animal weighing scale. Animals were weighed 1day before and on 1, 7, 14, 21 days after pMCAO and body weight changes were recorded.

2.5. Rat model of pMCAO surgery

Animals were fasted but with a water supply the night before surgery. The rat model of pMCAO was established using a modified

method described previously (Arii et al., 2001; Longa et al., 1989; Nito et al., 2004). The rats were anesthetized with halothane (4% for induction, 1% for maintenance) in a mixture of nitrous oxide and oxygen (70%:30%, v/v). After anesthesia, a rectal probe was inserted and body temperature was maintained at 37 °C with a heating lamp. With the animal in a secure supine position, a midline incision was made and the left common carotid, external carotid and internal carotid arteries were exposed. A 4-cm length of 4–0 monofilament nylon suture with its tip rounded by briefly heating the end was used to occlude the middle cerebral artery. The nylon filament was advanced from the external carotid artery into the lumen of the internal carotid artery until a resistance was felt (18–20 mm), indicating occlusion of the middle cerebral artery. The nylon filament was allowed to remain in place to create a permanent model of focal cerebral ischemia. In sham-operated animals, the common carotid artery and external carotid artery were exposed and the incision was sutured without touching the internal carotid artery. The incision was sutured with sterile nylon surgical sutures. Post surgery, animals were housed in separate, clean cages and were monitored continuously until they regained consciousness and were able to move freely. A Bederson's score (Bederson et al., 1986) was adopted for whether the model was successfully established.

The evaluation was conducted when rats were awake Scores higher than 1 were considered to be a successful model. The standard were as follows: 0 point: no neurological deficit symptoms; 1 point: mild neurological deficit symptoms; 2 points, moderate neurological deficit symptoms; 3 points, severe neurological deficit symptoms; 4 points, can't walk spontaneously. The excluded criteria were as below: 1, Bederson's score = 0 or 4 points; 2, subarachnoid hemorrhage occurrence during craniotomy; 3, animals that died before the scheduled time. The evaluation was performed by an observer who was blinded to the experimental group.

2.6. Behavioral tests

All animals were operated on and tested in parallel. All testing was conducted from 9 a.m. to 11 a.m. and each test apparatus was cleaned thoroughly between animals at each time point. Testing procedure involved two persons, one person who did the surgery and was in charge of handling the animals according to group assignment and another one who has tested the animals and was not aware of groups' identity.

2.7. The open field test (OFT)

The open field test is commonly used for evaluating locomotor activity and some behavioral parameters 1, 7, 14 and 21 days after the surgery. The open field was placed in an isolated room, and under the same standardized conditions, with no objects or clues that could represent signals and alter patterns of behavior. The open field apparatus consisted of a square area (100 × 100 cm) with walls 100 cm high that was made of gray polyvinylchloride plastic board. Center and periphery areas were further subdivided for assessment of overall locomotor activity. The zones were defined by dividing the open field were divided into a 4 × 4 grid using Etho Vision XT software (Noldus information technology, Wageningen, Netherlands), with each square measuring 25 × 25 cm. Thus, the center was the innermost 4 squares and the perimeter consisted of the squares on the edge of the field. The rats were placed in the center of the open-field for each 10 min trial while their activity was tracked by an overhead surveillance camera. Before testing animals were acclimated to a nearby dark holding room for 45 min and the test apparatus was cleaned between trials. Movements were tracked using custom image tracking software Etho Vision XT software connected to a video camera (Canon, Japan). The following behavioral parameters were recorded: (a) total travel distance(m); (b) mean velocity (cm/s); a-d they were measured automatically by a tracking program (Etho Vision XT software (Noldus information technology, Wageningen, Netherlands).

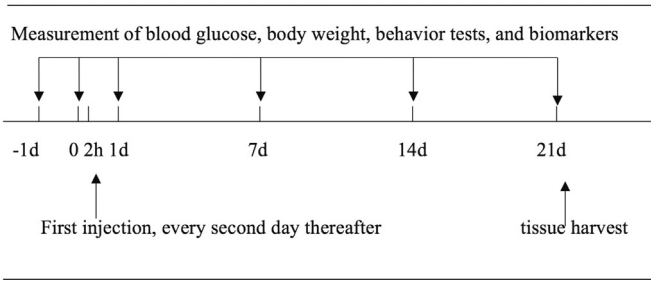

Fig. 1. Schematic representation of the study design.

2.8. Beam walking test

The beam-walking test was used to assess deficits in coordination and integration of motor movement, especially in the hindlimb. The rats were trained for three days to traverse the beam before ischemia induction and by the end of the training period all rats had learned the task. Beam walking test was performed on postoperative days 1, 7, 14 and 21. The ratio scale was modified from Ohlsson (Ohlsson and Johansson, 1995) and Feeney (Feeney et al., 1982). Briefly, rats were trained to walk on a wooden beam (100 cm long × 25 cm width) that was elevated 60 cm above the floor for 3 days consecutively before MCAO. After MCAO, beam walking tests were conducted with the following scoring system: 0, the rat falls down and cannot walk on the beam; 1, the rat is unable to walk on the beam but can sit on the beam; 2, the rat falls down while walking; 3, the rat can traverse the beam, but the affected hind limb does not aid in forward locomotion; 4, the rat crosses the beam with more than 50% foot slips; 5, the rat traverses the beam with fewer than 50% foot slips; 6, the rat successfully crosses the beam with no foot slips.

2.9. Screen test

To measure the muscle tone, strength, stamina and balance, a net screen was used. The screen test was conducted on the 1st, 7th, 14th and 21st days after operation in a blinded fashion as follows (Fan et al., 2018): from the left, right and upper side, a thin strip of wood (25 cm) and a mounting bracket (80 cm) were used for the fixation of the screen (50 × 50 cm^2) with a grid mesh (1 × 1 cm^2) with foam-rubber cushion set at the bottom when it was used. Firstly, the screen was horizontally placed and the rats were put on the screen, and then one side of the screen was raised and the screen was slowly raised in 2 s to be a vertical position and kept for 5 s. The standards were as follows: 0 point, the forepaw was able to grasp the screen for 5 s without falling; 1 points, temporarily grasped the screen and descended a short distance without falling; 2 points, falling within 5 s; 3 points, falling immediately when the screen rolled around.

2.10. Hanging wire test

All rats were trained for behavioral test for 3 days before MCAO. The hanging wire test was used to measure griping and forelimb strength of the rats after ischemia induced brain injury as described previously (Hunter et al., 2000). The hanging wire test was performed on day 1,7,14 and 21 post MCAO surgery. The investigator who conducted MCAO surgery and evaluated neurological score was blinded to the treatment group. The testing apparatus consisted of a piece of twine 2 mm in diameter and 50 cm long tied tightly between two vertical poles and suspended 60 cm over a lightly cushioned landing pad. The rat was held by the tail and suspended over the twine near its midpoint, with the rat facing the investigator. When the rat grasped the twine with its forepaws, the investigator released the tail and began timing. The time (in s) until the animal fell was recorded. The cut off time was taken as 90 s.

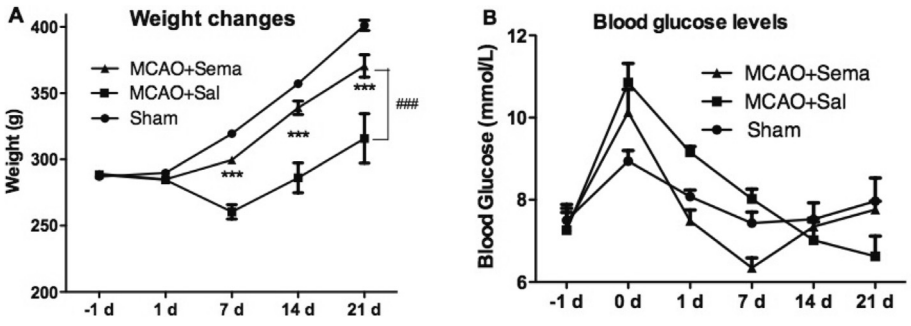

Fig. 2. A. Changes in rats' body weights, n = 12 per group. The difference of body weights among the three groups was statistically significant in an ANOVA test (### = $p < 0.001$). Post-hoc tests showed differences between groups: MCAO + Sal group and MCAO + Sema group compared with saline control (Sham); *** = $p < 0.001$, MCAO + Sema group compared with MCAO + Sal group. # = $p < 0.05$, ## = $p < 0.01$, ### = $p < 0.001$, MCAO + Sema group and MCAO + Sal group vs. Sham; * = $p < 0.05$, ** = $p < 0.01$, *** = $p < 0.001$ MCAO + Sema group vs. MCAO + Sal group.
2B. There is no statistical difference in glucose levels between the three groups ($F = 0.940$, $p > 0.05$).

2.11. Grip strength test

Grip strength tests originally characterized by Pin-Barre (Pin-Barre et al., 2014) were conducted on the 1st, 7th, 14th and 21st days post operation. For grip strength, animals were trained for the grip test before the experiment. During the tests, rats gripped the tension bar of the instrument (Ugo basile, Cat. No. 47200–327, Italy) using their forelimbs, and researchers held the tension plate using their right hands and tugged on the rat tails using their left hands. Next the researchers loosened their right hand grip and pulled back the rat body until the forelimbs slipped from the tension bar. Maximum tension values were recorded as effective data. Each rat was tested three times.

2.12. Immunohistochemistry

At different time points after pMCAO, rats were transcardially perfused with ice cold heparinized saline, followed by 4% paraformaldehyde, then the brains were removed. Hippocampal region of the brain tissues were fixed in 4% paraformaldehyde for 24–48 h, and embedded in O.C.T. Tissue Freezing Medium, (SAKURA Tissue-Tek® O.C.T. Compound, Order Number 4583). Immunofluorescence staining was used to detect DCX + cells in the hippocampal dentate gyrus at 1,7, 14 and 21 days after MCAO surgery. Brains were postfixed in 4% paraformaldehyde overnight, immersed in 20% and 30% sucrose until they were observed to sink to the bottom. Serial hippocampal sections (8 μm) were made on a cryostat (Leica Biosystems, Germany). Following hydration, a short cycle of mild antigen retrieval (pH = 6, 10 min in hot citrate buffer) and incubation of the sections with 10% fetal bovine serum containing 0.3% Triton X-100 for 1 h at room temperature. Then they were incubated overnight at 4 ˚C with primary antibody against the early neurogenesis marker DCX (1:100, Abcam, ab207175), in PBS. On the next day, the sections were washed 3 times in PBS for 10 min each and then incubated for 1 h at room temperature with fluorochrome-coupled secondary antibody (1:200; Alexa Fluor 594, Abcam, ab150080). The sections were then washed 3 times in PBS for 10 min each and incubated with 4′,6-diamidino-2-phenylindole (DAPI; Beyotime, C1005) for 10 min at room temperature. Negative controls received an identical treatment except for the primary antibody and showed no positive signal. Recording, storing, viewing and analyzing macroscopic images is made possible by 3DHISTECH's hardware and software tools (3DHISTECH Ltd, Hungary).

All DCX-positive cells were counted in both the ipsilateral and contralateral dentate gyrus. For the dentate gyrus, every 50th coronal section was selected from each rat for a total of 3 sections between anteroposterior + 5.86 mm and anteroposterior + 2.96 mm of the granule cell layer. DCX-positive cells in the dentate gyrus were counted in each section of three consecutive views (× 400) and presented as the number of the cells per square millimeter (mean ± SE). Density values for the 3 sections (dentate gyrus) were averaged to obtain a mean density value for each animal. The index of positive cells was calculated (number of each positive cell/number of DAPI-stained cells × 100).

For the analysis of other biomarkers, paraffin sections (4-μm-thick) were dewaxed and boiled, at ~95 ˚C for 15 min, in citrate buffer (Boster, China) for antigen retrieval. Then brain sections were blocked in 3% H_2O_2, 5% normal bovine serum albumin (BSA), and incubated with Iba-1 rabbit monoclonal antibody (1:1000,Abcam, ab178847) for microglia and NeuN rabbit monoclonal antibody (1:1000,Abcam,ab177487) for mature neurons in 0.1 mol/L PBS at 4 ˚C overnight. The secondary antibodies, secondary biotinylated conjugates and 5% BSA were from SABC-POD (rabbit IgG) kit (Boster, China). The slides were incubated with SABC for 30 min followed by biotinylated goat anti-rabbit antibody for 30 min at 37 ˚C. After each incubation, sections were thoroughly washed with phosphate buffered solution. Bound biotinylated antibodies were visualized using diaminobenzidine (DAB, Boster, China). Expression of target protein was considered positive when a brown staining pattern was observed. Sections incubated in the absence of primary antibody were used as negative controls. Sections were mounted with neutral resin. Recording, storing and viewing macroscopic images is made possible by 3DHISTECH's hardware and software tools (3DHISTECH Ltd, Hungary). Images were analyzed using Image J software (NIH, Bethesda MD, USA) by blinded investigators.

2.13. Cell counting

To examine the effects of semaglutide on MCAO-induced activation of microglia, Iba-1 was used as a microglial marker. NeuN was used as a baseline marker for mature neurons. The number of NeuN-positive or Iba-1-labelled cells was calculated within different hippocampal areas (stratum radiatum for CA1 and CA3, and dentate gyrus) from three rats per group. For each sample, three consecutive slices (thickness: 4 μm) were observed. First, the positive cells of each slice were counted in six randomly selected microscopic fields (1.0 mm^2 each) of different hippocampal (3 images from the left hippocampus and 3 images from the right hippocampus) areas under a 400 × light microscope. Then the average positive cells of each slice was obtained by counting the positive cells of each visual field, summing all the six fields, and then divided it by the number of visual fields. At last, the total average positive cells of each sample were calculated using the same method, and then used for statistical analysis.

2.14. Western blot analysis

At different time points after pMCAO, the rats were decapitated under excessive ether anesthesia. Hippocampal tissues were isolated and stored at −80 ˚C. Hippocampus were homogenized, and total protein was extracted using protein extraction kit (Boster, China) follow the protocol. The concentrations of proteins were determined by BCA kit (Boster, China). An aliquot of 20 μg of total protein from each sample was separated by 10%–12% SDS-polyacrylamide gel electrophoresis, then transferred onto a polyvinylidene difluoride membrane

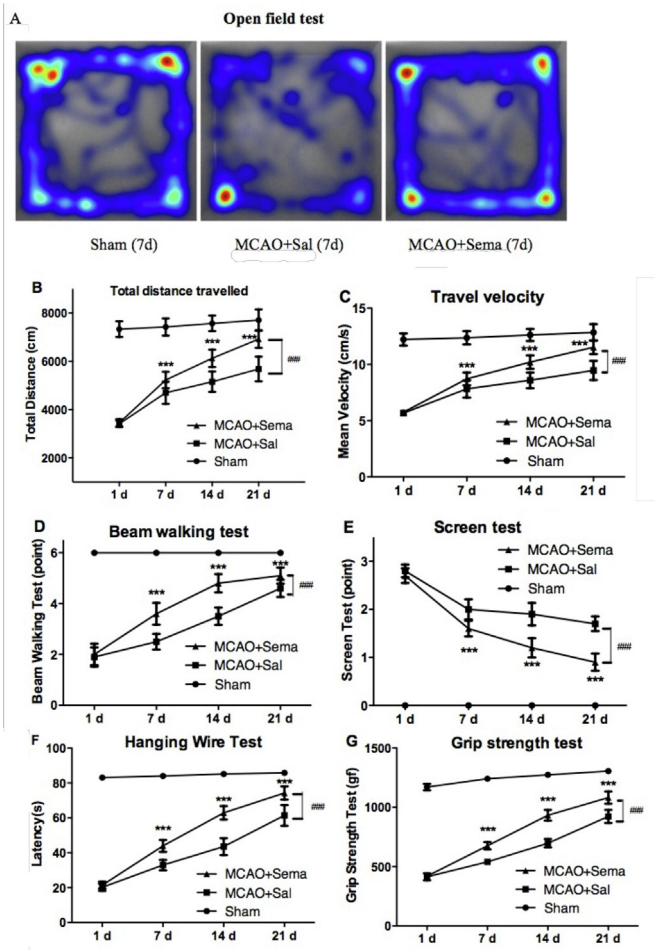

Fig. 3. A: Heat map of the rats' movements on day 7. **(B):** Compared with the sham group, rats in MCAO + Sal and MCAO + Sema group had decreased total travel distance (P < 0.001) at each time point. At day 7, 14 and 21, the total travel distance of rats in MCAO + Sema group is greater than that of rats in MCAO + Sal group significantly ($p < 0.001$). ### = $p < 0.001$, MCAO + Sal group and MCAO + Sema group compared with saline control (Sham); *** = $p < 0.001$, MCAO + Sema group compared with MCAO + Sal group. **(C):** Compared with the sham group, rats in MCAO + Sal and MCAO + Sema group had decreased mean velocity (P < 0.001) at each time point. At day 7, 14 and 21, the mean velocity of rats in MCAO + Sema group is faster than that of rats in MCAO + Sal group significantly ($p < 0.001$). ### = $p < 0.001$, MCAO + Sal group and MCAO + Sema group compared with saline control (Sham); *** = $p < 0.001$, MCAO + Sema group compared with MCAO + Sal group.

2C. Compared to sham group, the beam walking test scores in rats of MCAO + Sal and MCAO + Sema group decreased significantly (### = $p < 0.001$). There was no statistical difference between MCAO + Sal group and MCAO + Sema group on the first day ($p > 0.05$). Note the significant improvement in beam walking of Semaglutide-treated animals vs saline treatment group after ischemia at day 7, 14 and 21 (*** = $p < 0.001$). ### = $p < 0.001$, MCAO + Sal group and MCAO + Sema group compared with saline control (Sham); *** = $p < 0.001$, MCAO + Sema group compared with MCAO + Sal group.

D. Compared to sham group, the screen test scores in rats of MCAO + Sal group and MCAO + Sema group increased significantly (### = $p < 0.001$). There was no statistical difference between MCAO + Sal group and MCAO + Sema group on the first day ($p > 0.05$). Note the significant decline in screen test of Semaglutide-treated animals vs saline treatment group after ischemia (*** = $P < 0.001$) at day 7,14 and 21. ### = $p < 0.001$, MCAO + Sal group and MCAO + Sema group compared with saline control (Sham); *** = $p < 0.001$, MCAO + Sema group compared with MCAO + Sal group.

E. Dynamic changes in hanging wire test. Hanging wire scores of rats in the MCAO + Sal and MCAO + Sema groups were reduced significantly at day 1 and subsequently increased compared with sham ($p < 0.001$), but there is no significant difference between the two groups at day 1 ($p > 0.05$). After day 7, the difference of hanging wire scores between the MCAO + Sal and MCAO + Sema group was statistically significant ($p < 0.001$). ### = $p < 0.001$, MCAO + Sal group and MCAO + Sema group compared with saline control (Sham); ***$p < 0.001$, MCAO + Sema group compared with MCAO + Sal group.

= $p < 0.001$, MCAO + Sema group and MCAO + Sal group vs. Sham; *** = p < 0.001 MCAO + Sema group vs. MCAO + Sal group.

F. Dynamic changes in grip strength test. Grip strength of rats in the MCAO + Sal and MCAO + Sema groups were reduced significantly at day 1 and subsequently increased compared with sham ($p < 0.001$), but there is no significant difference between the two groups at day 1 ($p > 0.05$). Since day 7, the difference of grip strength between the MCAO + Sal group and MCAO + Sema group was statistically significant ($p < 0.001$). ###$p < 0.001$, MCAO + Sal group and MCAO + Sema group compared with saline control (Sham); ***$p < 0.001$, MCAO + Sema group compared with MCAO + Sal group. N = 12 per group.

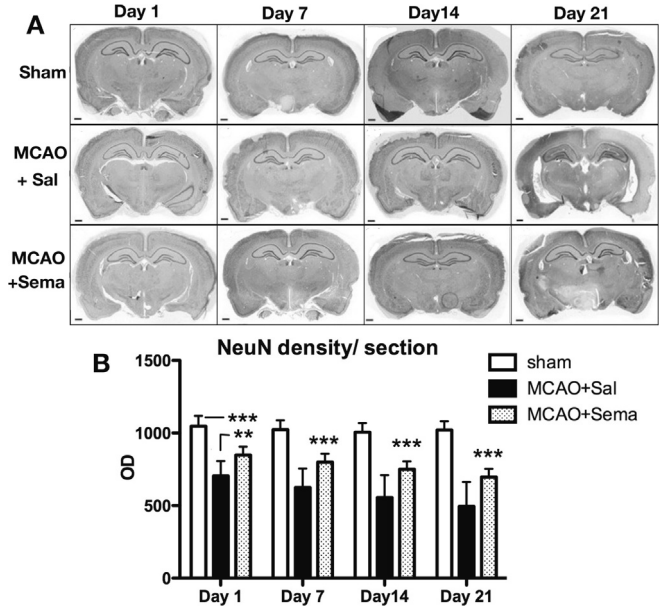

Fig. 4. Neuronal nuclear antigen (NeuN) staining. **(A)** NeuN density in the rat brain section after pMCAO. **(B)** All values were expressed as means ± SD. ** = p < 0.01 MCAO + Sema group compared with sham control group. *** = p < 0.001 compared with MCAO + Sal and sham control group. All groups N = 12. Scale bar = 1 mm.

(Millipore, USA). The membranes were blocked for 2 h in 5% BSA at room temperature. Then, the membranes were incubated for overnight at 4 °C (1 : 1000 dilution) with primary antibodies: MAPK p38 (Cell Signaling Technology, 8690S,USA), MKK7 (CellSignaling Technology, 4172S, USA), c-Raf (Cell Signaling Technology, 53745S,USA), ERK2 (Abcam, ab32081) c-Jun (Abcam, ab40766), caspase-3 (Abcam, ab184787), BCL-2 (Abcam,ab59348), Bax (Abcam, ab32503), and NF-kB p65 (Abcam, ab32536), SDF-1 (Abcam, ab25117), CXCR4 (Abcam, ab197203),DCX (Abcam, ab207175), Nestin (Abcam, ab6142), IRS (Cell Signaling Technology, 3407S, USA), p-IRS (Cell Signaling Technology, 2385S, USA), ERK1/2 (Cell Signaling Technology, 8544S,USA), and p-ERK1/2 (Cell Signaling Technology, 4370S, USA) in diluents buffer. After washed with TBST, the membrane was incubated with HRP-conjugated secondary antibodies against rabbit IgG (1 : 5000 dilution) at room temperature for 2 h. Protein expression was tested by an enhanced chemiluminescence (ECL) method and visualized by ChemiDoc™ XRS+ (BIORAD, Hercules, CA, USA). Band patterns were analyzed with Image J software (National Institutes of Health, USA). The densitometric values were normalized with respect to the values of β-actin immunoreactivity to correct for any loading and transfer differences between samples. Each experiment was repeated three times,

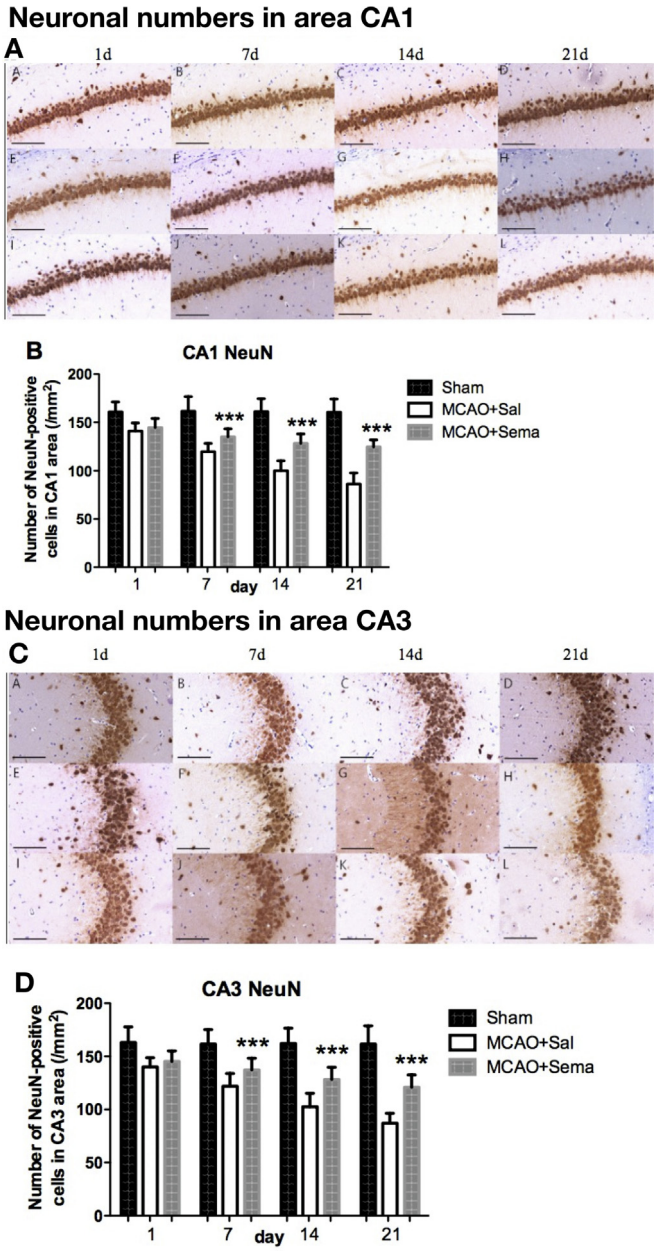

Fig. 5. Neurodegeneration in the CA1 layer of hippocampus 1 (A,E,I), 7 (B,F,J), 14 (C,G,K) and 21 (D,H,L) days after ischemia. **(A)** Representative photographs of the CA1 hippocampal layer NeuN-immunostained, sham group. (A–D), MCAO + Sal(E-H) and MCAO + Sham (I–L) rats showing degeneration of neurons and decrease in the number of neurons at 400 × magnification. **(B).** The number of NeuN-immunostained neurons in the CA1 layers. Treatment with semaglutide attenuated hippocampal neuronal loss by ischemia in the CA1 layers. ***$p < 0.001$, MCAO + Sema group compared with MCAO + Sal group. N = 3 per group, scale bar = 100 μm. Neurodegeneration in the CA3 layer of hippocampus. **(C)** Representative photographs of the CA3 hippocampal layer NeuN-immunostained, in sham (A-D), MCAO + Sal (E–H) and MCAO + Sham (I-L) rats 1 (A,E,I), 7 (B,F,J), 14 (C,G,K) and 21 (D,H,L) days after ischemia. N = 3 per group, scale bar = 100 μm. **(D).** The number of NeuN-immunostained neurons in the CA3 layers. Treatment with semaglutide attenuated hippocampal neuronal loss by ischemia in the CA3 layers. *** = $p < 0.001$, MCAO + Sema group compared with MCAO + Sal group.

and the results are presented as mean ± SD. (See. Fig. 1)

2.15. Statistical analysis

Data were performed using SPSS 16.0 software. All of the values are presented as the mean ± SD and were analyzed using a two-way analysis of variance (ANOVA) with treatment (Sham, MCAO + sal, MCAO + Sema) and day (baseline, days 1,7, 14, 21) serving as the two factors. To detect significant differences among the experimental groups and days, ANOVAs were supported by the Bonferroni post-hoc tests. A Bonferroni correction was used for any multiple comparisons. P values < 0.05 were considered statistically significant.

3. Results

3.1. Body weight changes

The body weight of the rats in the control group showed an increasing trend. After stroke, the body weight declined at day 1, there was no statistical difference in the body weight of the rats among each group ($p > 0.05$). Compared with the sham group, the weight loss in MCAO + Sal group was obvious at day 7, then slowly increased. Compared with the MCAO + Sal group, the MCAO + Sema group gained more weight at day 7,14 and 21, and the difference among these three group is statistically significant ($F = 22.624$, $p < 0.001$) (Fig. 2A).

3.2. Blood glucose levels

The blood glucose levels of the rats in the control group had no obvious changing at each time point ($p > 0.05$). Compared with the control, after stroke blood glucose increased in the MCAO + Sal group and MCAO + Sema group, then drops. After day 7, blood glucose levels in MCAO + Sema group are gradually returning back to normal, and blood sugar levels in MCAO + Sal group continue to fall until day 21. There is no statistical difference among these three groups ($F = 0.940$, $p > 0.05$) (Fig. 2B).

3.3. Open field assessment

The total exercise distance and mean velocity of the rats in sham group had no statistically significance at each time point ($p > 0.05$). Rats in MCAO + Sal group had decreased total travel distance ($p < 0.001$, Fig. 3B), and decreased mean velocity ($p < 0.001$, Fig. 3C), compared to the Sham group at each time point. On the first day after stroke, there was no significant difference in total exercise distance and mean velocity between MCAO + Sal group and MCAO + Sema group ($p > 0.05$). At day 7, 14, and 21, the total travel distance and mean velocity of the rats in MCAO + Sal group improved slowly compared with the MCAO + Sema group ($p < 0.001$). There was a significant difference of the total exercise distance and mean velocity among the three groups ($F = 41.067$,$p < 0.001$).

3.4. Beam walking test

The beam walking test results showed that score was significantly lower in the MCAO + Sal group and MCAO + Sema group than that in the sham group at each time point ($p < 0.001$); while the score was obviously higher in MCAO + Sema group than that in the MCAO + Sal group at the 7th, 14th and 21st days ($p < 0.001$). There was significant difference of beam walking scores among the three groups ($F = 29.930$, $p < 0.001$) (Fig. 3D).

3.5. Screen test

Screen test results showed that the scores in MCAO + Sal group and

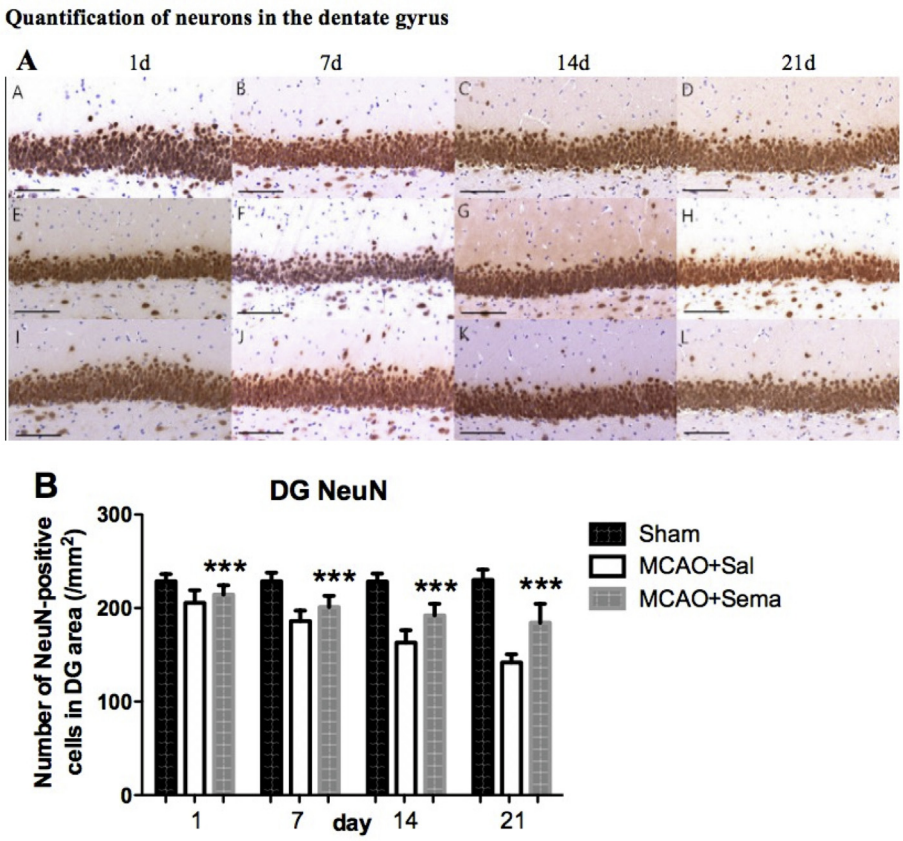

Fig. 6. Neurodegeneration in the dentate gyrus. **(A)** Representative photographs of the DG hippocampal layer NeuN-immunostained, in sham (A–D), MCAO + Sal (E–H) and MCAO + Sham (I–L) rats 1 (A,E,I), 7 (B,F,J), 14 (C,G,K) and 21 (D,H,L) days after ischemia at 400 × magnification. **(B).** The number of NeuN-immunostained neurons in the dentate gyrus layers. Treatment with semaglutide attenuated hippocampal neuronal loss by ischemia in the DG layers. ***$p < 0.001$, MCAO + Sema group compared with MCAO + Sal group. N = 3 per group, Scale bar = 100 μm.

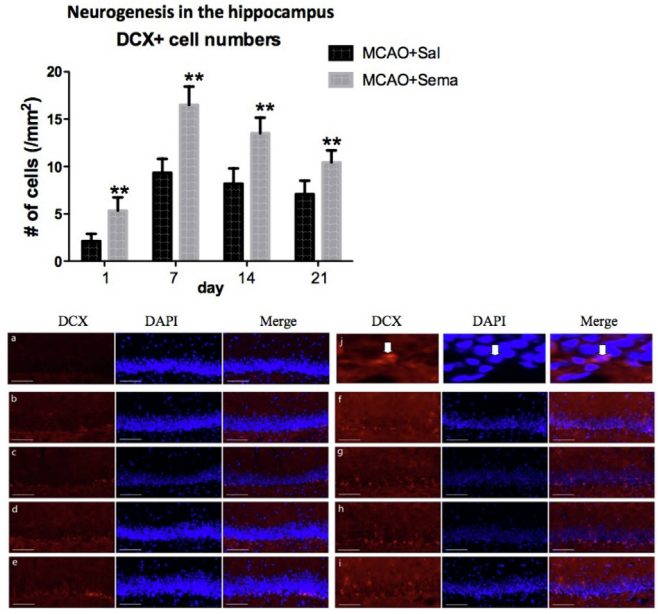

Fig. 7. Time course of doublecortin (DCX) expression in cells of the adult dentate gyrus. ** = $p < 0.01$, MCAO + Sema group compared with MCAO + Sal group. Sample images are shown below: Cellular colocalization of doublecortin (DCX) immunoreactivity. DCX (red) and nucleus marker DAPI (blue) in the dentate gyrus (a–i). a:Sham,b:MCAO + Sal(1d), c: MCAO + Sal (7d) d: MCAO + Sal (7d); e: MCAO + Sal(21d); f:MCAO + Sema (1d); g: MCAO + Sema (7d); h: MCAO + Sema (14d); i: MCAO + Sema (21d); (j) DCX/DAPI double-positive cell at 400 × magnification. N = 3 per group, scale bar = 100 μm. (For interpretation of the references to colour in this figure legend, the reader is referred to the web version of this article.)

MCAO + Sema group was found higher than that in the sham group ($p < 0.001$). Compared with MCAO + Sal group, the decline of screen test scores in rats of MCAO + Sema group is greater ($p < 0.001$) since 7 days after ischemia. There was significant difference of screen test scores among the three groups (F = 106.525, $p < 0.001$) (Fig. 3E).

3.6. Hanging wire grip test

The hanging wire scores of the rats in the sham group are similar for each time point ($p > 0.05$). Compared with the sham group, the scores decreased significantly in the MCAO + Sal group and MCAO + Sema group in day 1, then increased gradually ($p < 0.001$). The improvement of hanging wire scores in the MCAO + Sema group is more significant than in MCAO + Sal group since day 7 ($p < 0.001$). There is statistical difference among these three groups (F = 106.525, P < 0.001) (Fig. 3F).

3.7. Grip strength test

The grip strength of the rats in the sham group had no obvious changing at each time point ($p > 0.05$). Compared with the sham, the strength decreased significantly in the MCAO + Sal group and MCAO + Sema group in day 1 and then increased gradually ($p < 0.001$). The growth of strength in the MCAO + Sema group is more significant than in MCAO + Sal group since day 7 ($p < 0.001$). There is a statistical difference among these three groups (F = 118.982, P < 0.001) (Fig. 3G).

3.8. Neurogenesis, (neuroblast proliferation)

There was no obvious double-cortin (DCX)-positive cell expression in the sham group. Examples of co-labeling of DCX-positive cells with DAPI are depicted in Fig. 7. We quantified the number of DCX-positive

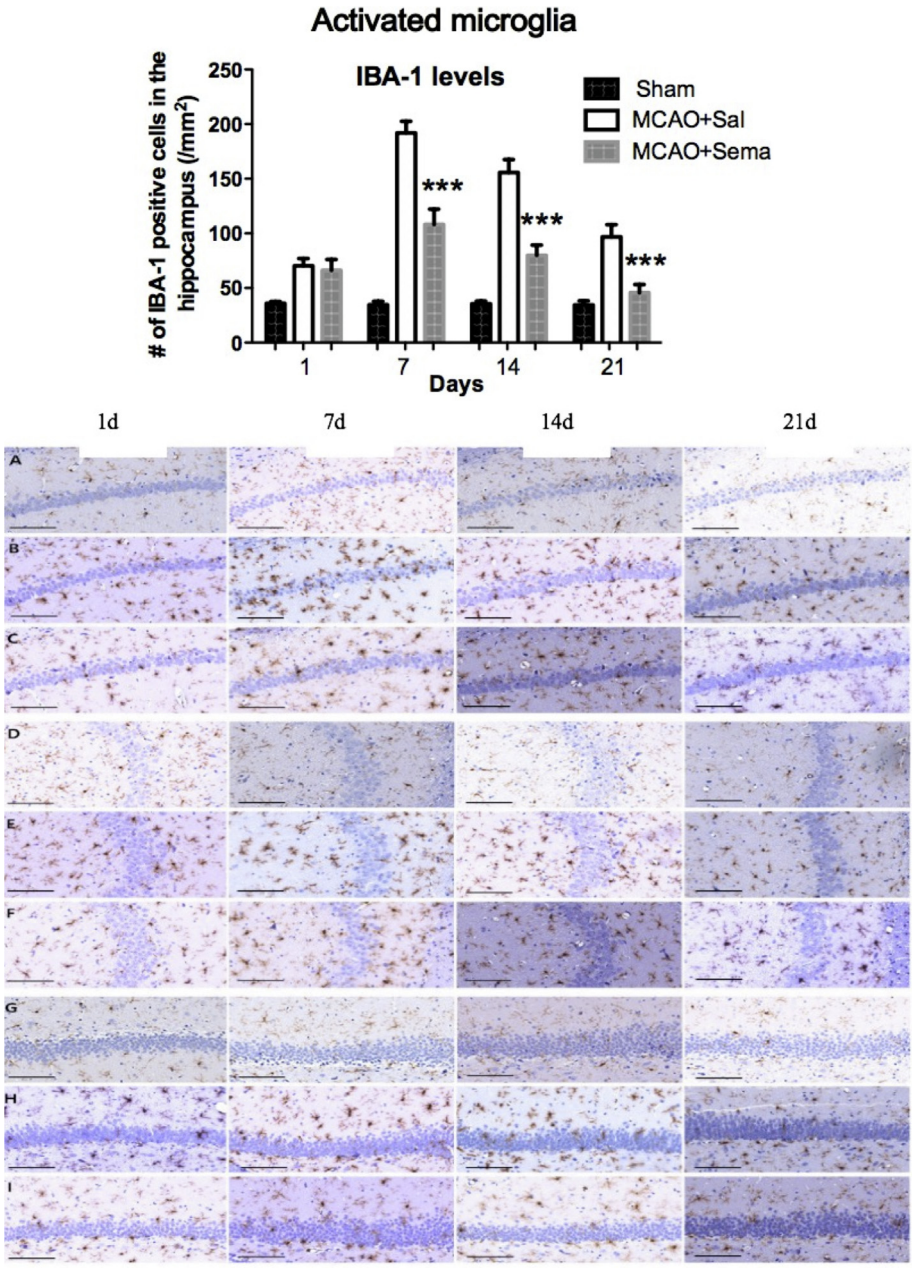

Fig. 8. Ischemia increased the number of activated microglial cells (IBA-1 stain). Treatment with semaglutide attenuated microglial activation in the hippocampus. *** = $p < 0.001$, MCAO + Sema group compared with MCAO + Sal group. Sample images are shown below. IBA-*l*-1positive microglia in the CA1, CA3, and DG regions of the hippocampus in rats. Representative photomicrographs of level-matched coronal sections of hippocampal formation CA1 (A–C), CA3 (D–F) and DG (G–I), from control (A, D, G), MCAO + Sal (B, E, H) and MCAO + Sema (C, F, I) rats at 400 × magnification. N = 3 per group, scale bar = 100 μm.

cells in the dentate gyrus after MCAO. The numbers of DCX-positive cells began to rise on the 1st day, and peak on the 7th day, then the numbers gradually decreased in MCAO + Sal group and MCAO + Sema group. Compared with MCAO + Sal group, the numbers of DCX-positive cells in MCAO + Sema group is higher ($F = 25.277$, $p < 0.01$) at each time point.

3.9. Activated microglia, Iba-1 expression in the hippocampus

The numbers of Iba-1-positive cells in the hippocampus showed significant group differences ($F = 2386.8$, $P < 0.001$). In sham-operated animals, no significant differences were found at each time point. Ischemia increase expression of Iba-1 in the hippocampus since day 7: the Iba-1 positive cell number was significantly higher in the MCAO + Sal and MCAO + Sema than in the control group ($p < 0.001$). Treatment with semaglutide significantly reduced the numbers of Iba-1-positive cells in the hippocampus of ischemic animals. The MCAO + Sema group showed a significantly lower number of Iba-1 positive cells compared to the MCAO + Sal since day 7 ($p < 0.001$). Fig. 8.

3.10. Lesion size and neuronal numbers in the hippocampus

When analyzing NeuN immunostaining over the whole brain section which represents the neuronal loss, a difference between sham controls and MCAO + sal and MCAO + Sema groups was found. A difference between MCAO + sal and MCAO + Sema groups was found (Fig. 4). When quantifying neuronal numbers, Neurodegeneration in the hippocampus showed significant group effects in different regions of the hippocampus ($P < 0.001$). Compared to control rats, the number of

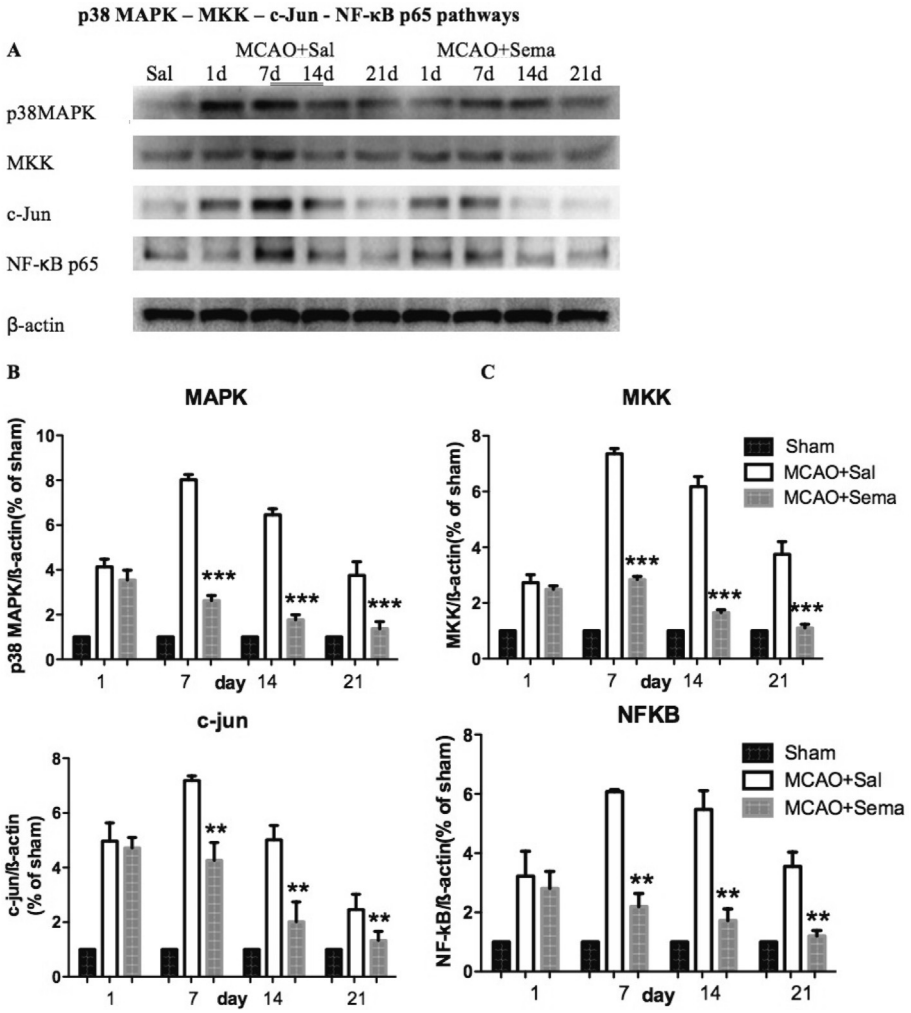

Fig. 9. Effects of semaglutide on the expression of pro-inflammatory cytokines, p38 MAPK, MKK, c-Jun, and NF-κB p65 activation, induced by ischemia. N = 3. **(A)** Sample Western blot bands. **(B)** Western blot analysis for the expression of p38 MAPK. *** = $p < 0.001$, MCAO + Sema group compared with MCAO + Sal group. **(C)** Levels of MKK. *** = $p < 0.001$, MCAO + Sema group compared with MCAO + Sal group. **(D)** Levels of c-Jun. ** = $p < 0.01$ MCAO + Sema group compared with MCAO + Sal group. **(E)** Levels of NF-κB p65. ** = $p < 0.01$, MCAO + Sema group compared with the MCAO + Sal group.

NeuN-positive neurons in the CA1 (Fig. 5A and B), CA3 (Fig. 5C and D) and DG (Fig. 6) region decreased in MCAO + Sal and MCAO + Sema groups ($p < 0.001$). Semaglutide increased hippocampal neuronal survival post ischemia. In the CA1 and CA3 region, the number of NeuN-positive neurons in MCAO + Sema group was larger than in the MCAO + Sal group since day 7 ($p < 0.001$); In the DG region, the number of NeuN-positive neurons in MCAO + Sema group was larger than in the MCAO + Sal group since day 1 ($p < 0.001$).

3.11. The p38 MAPK – MKK – c-Jun- NF-κB p65 inflammation signaling pathway

(1) p38 MAPK:The expression of p38 MAPK showed a significant difference between groups (F = 311.834, p < 0.001). Compared with the sham group, the expression of p38 MAPK in the MCAO + Sal group and MCAO + Sema group increased (p < 0.001), it began to rise on the first day, peaked on the seventh day, and then declined. Compared with the MCAO + Sal group, the expression of p38 MAPK in MCAO + Sema group decreased since day 7 (p < 0.001). See Fig. 9.

(2) MKK: The expression of MKK showed a significant difference between groups (F = 248.856, p < 0.001). Compared with the sham group, the expression of MKK in the MCAO + Sal group and MCAO + Sema group increased (p < 0.001), it began to rise on the first day, peaked on the seventh day, and then declined. Compared with the MCAO + Sal group, the expression of MKK in MCAO + Sema group decreased since day 7 (p < 0.001) (Fig. 9C).

(3) c-Jun: The expression of c-Jun showed a significant difference between groups (F = 97.954,p = 0.001). Compared with the sham group, the expression of c-Jun in the MCAO + NS group and MCAO + Sema group increased (p < 0.001), began to rise on the first day, peaked on the seventh day, and then declined. Compared with the MCAO + Sal group, the expression of c-Jun in MCAO + Sema group decreased since day 7 (p < 0.01) (Fig. 9D).

(4) The expression of NF-κB p65 showed a significant difference between groups (F = 68.168; P = 0.001). Compared with the sham group, the expression of NF-κB p65 in the MCAO + Sal group and MCAO + Sema group increased (p < 0.01), it began to rise on the first day, peaked on the seventh day, and then declined. Compared with the MCAO + Sal group, the expression of NF-κB p65 in MCAO + Sema group decreased significantly at day 7, day14, and day 21 (p < 0.01) (Fig. 9E).

3.12. Apoptosis signaling pathway: C-raf, ERK2, Bcl-2/BAX and Caspase-3 levels

(1) C-raf: The expression of C-raf showed a significant difference between groups (F = 15.862,P = 0.016). Compared with the sham

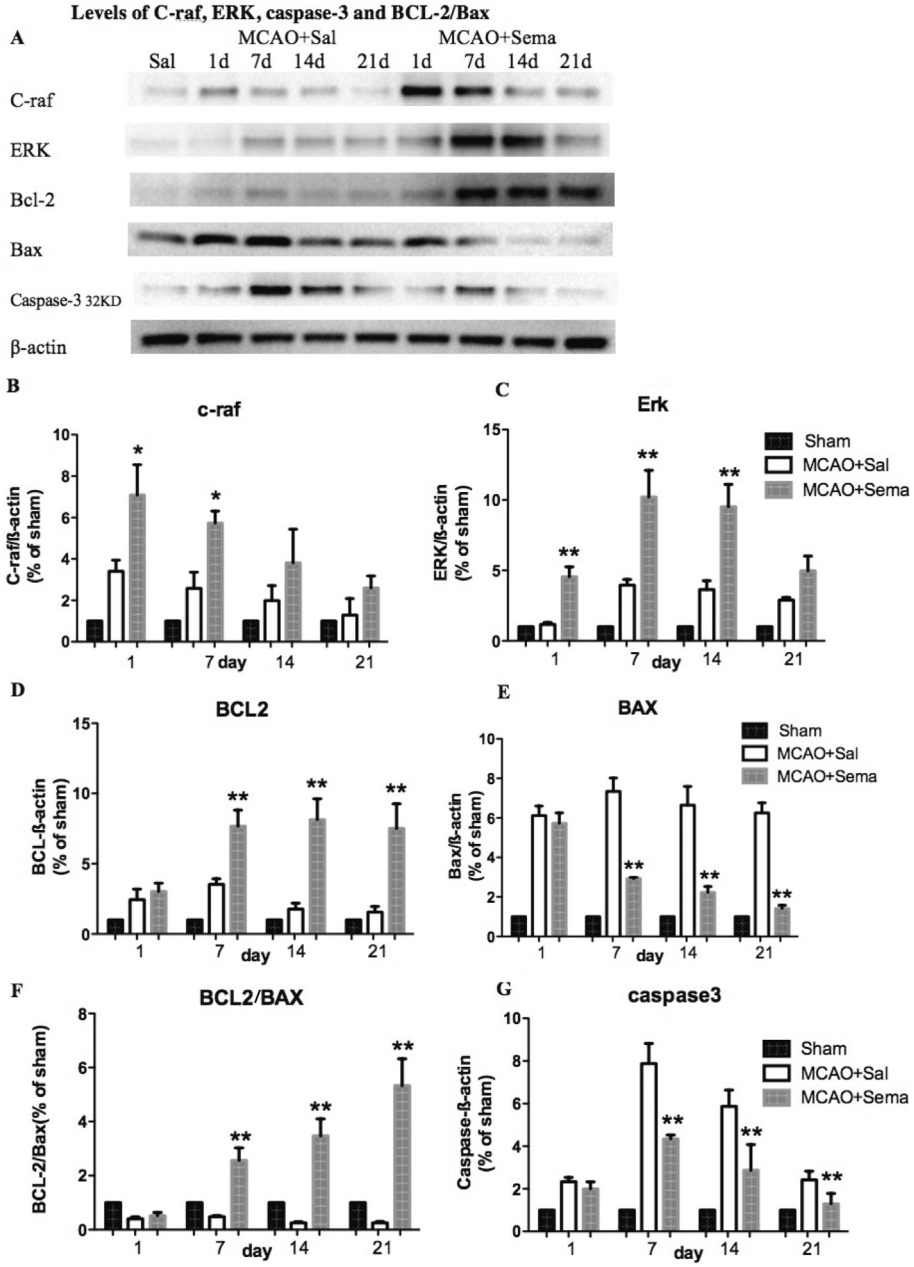

Fig. 10. Effects of semaglutide on the expression of C-raf, ERK, caspase-3 and BCL-2/Bax activation, induced by ischemia. **(A)** Sample Western blot bands. N = 3. **(B)** Levels of C-raf. * = $p < 0.05$, MCAO + Sema group compared with MCAO + Sal group. **(C)** Levels of ERK. ** = $p < 0.01$, MCAO + Sema group compared with MCAO + Sal group. **(D)** Protein levels of BCL-2. ** = $p < 0.01$, MCAO + Sema group compared with the MCAO + Sal group. **(E)** Levels of Bax. ** = $p < 0.01$, MCAO + Sema group compared with the MCAO + Sal group. **(F)** Ratio of BCL-2/Bax levels. ** = $p < 0.01$, MCAO + Sema group compared with the MCAO + Sal group. **(G)** Levels of Caspase-3. ** = $p < 0.01$, MCAO + Sema group compared with MCAO + Sal group.

group, the expression of C-raf in the MCAO + Sal group and MCAO + Sema group increased ($p < 0.05$), it peaked on the first day, and then declined. Compared with the MCAO + Sal group, the expression of C-raf in MCAO + Sema group increased more significantly at day 1 and day 7 ($p < 0.05$). Fig. 10.

(2) ERK2: The expression of ERK showed a significant difference between groups (F = 37.010,P = 0.004). Compared with the sham group, the expression of ERK in the MCAO + NS group and MCAO + Sema group increased ($p < 0.01$), it began to rise on the first day, peaked on the seventh day, and then declined. Compared with the MCAO + Sal group, the expression of ERK2 in MCAO + Sema group increased more significantly at day 1, day7 and day 14 ($p < 0.01$) (Fig. 10C).

(3) BCL-2/Bax: The levels of BCL-2(F = 31.801,P = 0.005) and Bax (F = 105.154 P = 0.001) showed a significant difference between groups, and the ratio of BCL-2/Bax showed a significant difference between groups (F = 70.737,P = 0.001). Compared with the sham group, the expression of BCL-2/Bax decreased at each time point ($p < 0.01$). Compared with the MCAO + Sal group, the expression of BCL-2/Bax in the MCAO + Sema group increased significantly at each time point (from day 7 onward) ($p < 0.01$) (Fig. 10D–F).

(4) Caspase-3: The expression of Caspase-3 showed a significant difference between groups (F = 24.581,P = 0.008). Compared with the sham group, the expression of Caspase-3 in the MCAO + Sal group and MCAO + Sema group increased ($p < 0.01$), it began to rise on the first day, peaked on the seventh day, and then declined. Compared with the MCAO + Sal group, the expression of Caspase-3 in MCAO + Sema group decreased significantly at day 7, day14 and day 21 ($p < 0.01$) (Fig. 10G).

3.13. Levels of growth factor kinase ERK1/2 and pERK1/2 and insulin receptor substrate IRS-1 and pIRS-1

The expression of ERK1/2 and p-ERK1/2 in the MCAO + NS group and MCAO + Sema group began to rise on the first day, and reached its peak on the 7th day, then declined. Compared with the MCAO + Sal

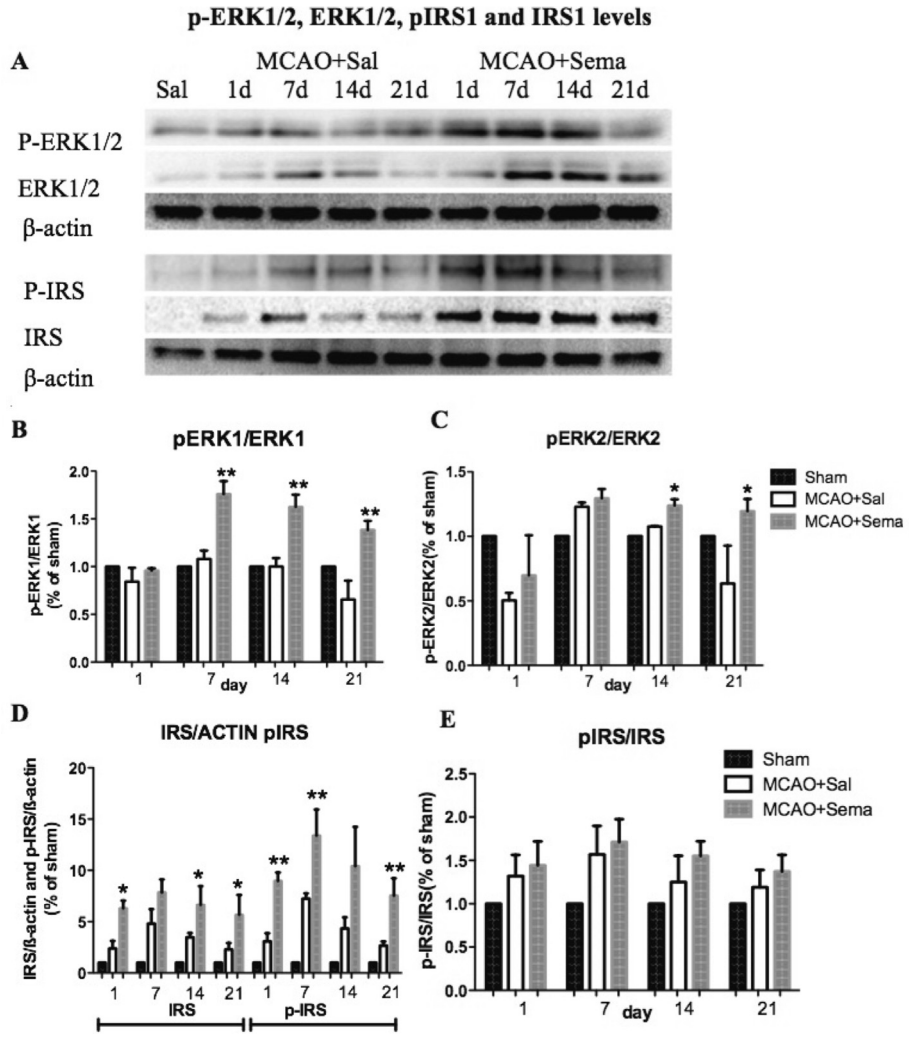

Fig. 11. Western blot analysis for the expression of ERK1/2, pERK1/2, p-IRS and IRS. N = 3. (A) sample Western blot bands. **(B)** Ratios of p-ERK1/ERK1 and **(C)** p-ERK2/ERK2. p-ERK1/ERK1: ** = $p < 0.01$, MCAO + Sema group vs. MCAO + Sal group. p-ERK2/ERK2: * = $p < 0.05$, MCAO + Sema group vs. MCAO + Sal group. **(D)** Expression of IRS and p-IRS levels. IRS:* = $p < 0.05$,MCAO + Semagroup vs. MCAO + Sal group. p-IRS:**$p < 0.01$, MCAO + Sema group vs. MCAO + Sal group. **(D)** Ratios of pIRS to IRS levels.

group, the expression of ERK2 ($p < 0.01$) and p-ERK2 ($p < 0.001$) in MCAO + Sema group increased more remarkably from day 7 on, and then gradually declined. The difference in the ratio of ERK1/p-ERK1 ($p < 0.01$) and ERK2/p-ERK2 ($p < 0.05$) between the two groups was statistically significant. It appears that semaglutide promotes the expression of ERK1/2 and p-ERK1/2. Fig. 11.

3.14. Levels of growth factor kinase ERK1/2 and pERK1/2 and insulin receptor substrate IRS-1 and pIRS-1

The levels of IRS and p-IRS in the model group in the MCAO + NS group and MCAO + Sema began to rise on the first day, peaked on the 7th day, then declined (Fig. 11A). Compared with the MCAO + NS group, the expression of IRS ($p < 0.05$) and p-IRS ($p < 0.01$) in the MCAO + Sema group increased at each time point. But the ratio of p-IRS/IRS between the two groups has no significant statistical difference ($p > 0.05$) (Fig. 11B).

3.15. Levels of neurogenesis biomarkers nestin, CXCR4, SDF-1, and DCX

(1) Nestin: The expression of nestin showed a significant difference between groups (F = 466.500, $p < 0.001$). Compared with the Sham group, the expression of nestin in the MCAO + Sal group and MCAO + Sema group increased ($p < 0.001$). The expression of nestin in the MCAO + Sal group began to rise on the first day, and reached its peak on the seventh day, then went down again. Compared with the MCAO + Sal group, the expression of nestin in the MCAO + Sema group reached its peak on the first day, which means that the peak of nestin expression is earlier, then it fell down slowly ($p < 0.001$. Fig. 12B.

(2) CXCR4:The expression of CXCR4 showed a significant difference between groups (F = 438.457, $p < 0.001$). Compared with the sham group, the expression of CXCR4 in the MCAO + Sal group and MCAO + Sema group increased ($p < 0.001$) began to rise on the first day, peaked on the seventh day, and then declined. Compared with the MCAO + Sal group, the expression of CXCR4 in MCAO + Sema group increased at each time point ($p < 0.001$) (Fig. 12C).

(3) SDF-1:The expression of SDF-1 showed a significant difference between groups (F = 33.499,$p = 0.004$). Compared with the sham group, the expression of SDF-1 in the MCAO + Sal group and MCAO + Sema group increased ($p < 0.01$), it began to rise on the first day, peaked on the seventh day, and then declined. Compared with the MCAO + Sal group, the expression of SDF-1 in MCAO + Sema group increased since day 7 ($p < 0.01$. (Fig. 12D).

(4) DCX: The expression of DCX showed a significant difference

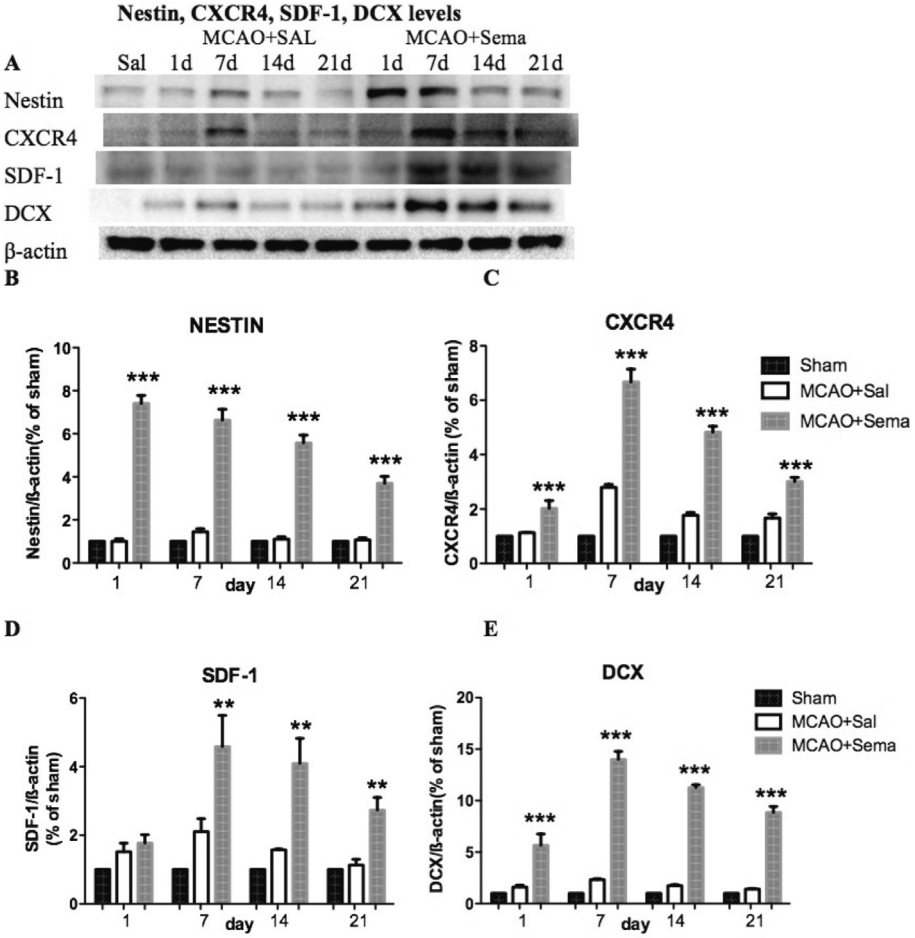

Fig. 12. Expression levels of neurogenesis markers. N = 3. **(A)** Sample Western blot bands. **(B)** Western blot analysis for the expression of Nestin.*** = $p < 0.001$, MCAO + Sema group compared with MCAO + Sal group. **(C)** Levels of CXCR4.***$p < 0.001$, MCAO + Sema group compared with the MCAO + Sal group. **(D)** Levels of SDF-1.**$p < 0.01$, MCAO + Sema group compared with the MCAO + Sal group. **(E)** Levels of DCX.***$p < 0.001$, MCAO + Sema group compared with the MCAO + Sal group.

between groups (F = 632.421, $p < 0.001$). Compared with the sham group, the expression of DCX in the MCAO + Sal group and MCAO + Sema group increased ($p < 0.001$), it began to rise on the first day, peaked on the seventh day, and then declined. Compared with the MCAO + Sal group, the expression of DCX in MCAO + Sema group increased at each time point ($p < 0.001$) (Fig. 12E).

4. Discussion

MCAO is a classical and well-characterized experimental model of cerebral ischemia (Longa et al., 1989). Our results document a range of protective effects of semaglutide in this animal model of stroke. The results demonstrate that in normoglycemic animals, GLP-1R agonists have no effect, and in non-obese animals, the effect on body weight is minimal (Feng et al., 2018; Jalewa et al., 2017). In clinical trials testing exenatide in non-obese and non-diabeticc PD patients, no noticeable effects were observed in body weight and blood glucose (Athauda et al., 2017).

Importantly, all motor tests showed improvement in motor control and muscle strength by drug treatment. Importantly, the expression of the biomarker IBA-1 in microglia and the activation of the pro-inflammatory second messenger cell signaling pathway p38 MAPK – MKK – c-Jun - NF-κB p65 was much reduced. This pathway is activated by pro-inflammatory cytokines such as TNF-α and activates a range of genes related to the inflammation response (Clark and Vissel, 2014). Importantly, it also inhibits growth factor signaling and activates pro-inflammatory cell signaling (Bomfim et al., 2012; Lee et al., 2010). Inflammation and apoptosis play an important role in cerebral ischemic pathogenesis (Qiao et al., 2012). It is well known that glial cells including astrocytes and microglia are activated by ischemic stroke and that the activated glia are involved in ischemia-induced neuronal death via the release of proinflammatory cytokines, reactive oxygen intermediates, and nitric oxide (Muir et al., 2007). NF-κB which plays a pivotal role in both inflammation and cell survival regulates a vast number of proinflammatory genes including IL-1, IL-6, TNF-α, and genes related to apoptosis such as Bcl-2, Bax and Fas (Malek et al., 2007). Bcl-2 family members such as Bax and Bad promote apoptosis, whereas, other members including Bcl-2 and Bcl-Xl exert anti-apoptosis effects. Bcl-2 heterodimerizes with Bax, thereby sequestering Bax and antagonizing the cell death-inducing activity (Yin et al., 1995). To our knowledge, our study is the first time to use pMCAO model to explore semaglutide's effect in ischemic injury and the role of the p38 MAPK – MKK – c-Jun pathway and C-raf – ERK –Caspase-3, BCL-2/Bax pathways in mediating the anti-inflammatory and anti-apoptosic effects. Semaglutide can prevent ischemia -induced neurotoxicity through suppression of p38 MAPK/MKK/c-Jun activity. Semaglutide can also increase the expressions of C-raf/ERK/BCL-2 and decrease the expressions of NF-κB, Caspase-3 and Bax to reduce apoptosis and neuronal death. Pro-inflammatory cytokines and p38 MAPK/MKK/c-Jun cell signaling furthermore block growth factor activity such as insulin and IGF-1 signaling (Hölscher, 2019; Talbot and Wang, 2014) The loss of growth

factor cell signaling results in reduced energy utilization, gene expression, cell growth and cell repair (Clark and Vissel, 2014; Holscher, 2014b; Neth and Craft, 2017). We show in this study that semaglutide can re-sensitize insulin signaling and normalize activity of the IRS1 and ERK1 cell signaling pathways. This improvement of growth factor signaling can also normalize stem cell proliferation and neurogenesis in the brain (Hunter and Holscher, 2012; Parthsarathy and Holscher, 2013). In selected brain areas such as the detate gyrus, neurogenesis continues in the adult brain and may be helpful in restoring function after a stroke. Trophic factors such as stromal cell-derived factor 1 alpha (SDF-1α) are upregulated in the ischemic brain, which promote endogenous regeneration (Chau et al., 2017), and CXCR4 is its receptor. Nestin is an intermediate filament protein which is expressed by immature cells and non-neural cell types (Daniel et al., 2008), particularly the neural progenitor cells (NPCs) (Sunabori et al., 2008) as well as microglia (Takamori et al., 2009). Nestin expression in the adult nervous system has been detected in a number of pathological conditions including cerebral ischemia (Duggal et al., 1997). Doublecortin (DCX) is a microtubule-associated protein expressed by neuroblasts and is considered to be a reliable marker of neurogenesis (Brown et al., 2003; Couillard-Despres et al., 2005). This protein is highly expressed in both cell body and dendrites of the newly generated neuroblasts. Expression of DCX is also associated with migration of neuronal precursors during development of the nervous system (Meyer et al., 2002). We were able to show in this study that levels of these biomarkers for neurogenesis are enhanced after MCAO, and that semaglutide treatment was capable of improving neurogenesis markedly. This may be an additional protective mechanism of this drug to help brain regeneration after stroke. What's more, we found that the peak expression of nestin was advanced to 1 day, after which the expression decreased gradually. As time is very important for neuronal survival in cerebral infarction, this early expression may contribute to the overall neuroprotective effect.

Post-semaglutide treatment robustly improved functional recovery of MCAO rats after ischemia without affecting blood glucose levels. Inflammation and apoptosis was reduced by the drug, and cell growth signaling and neurogenesis normalized. As semaglutide is already on the market as a treatment for diabetes, it is a promising candidate for drug repurposing and could be tested in clinical trials in stroke patients.

Conflicts of interest

The authors declare that there is no conflict of interest.

Acknowledgements

This study was supported by the Doctors Special Fund from the Second Hospital Affiliated to Shanxi Medical University (201801-6).

References

Ahren, B., 2014. Insulin plus incretin: a glucose-lowering strategy for type 2-diabetes. World J. Diabetes 5, 40–51.
Arii, T., Kamiya, T., Arii, K., Ueda, M., Nito, C., Katsura, K.I., Katayama, Y., 2001. Neuroprotective effect of immunosuppressant FK506 in transient focal ischemia in rat: therapeutic time window for FK506 in transient focal ischemia. Neurol. Res. 23, 755–760.
Athauda, D., Maclagan, K., Skene, S.S., Bajwa-Joseph, M., Letchford, D., Chowdhury, K., Hibbert, S., Budnik, N., Zampedri, L., Dickson, J., Li, Y., Aviles-Olmos, I., Warner, T.T., Limousin, P., Lees, A.J., Greig, N.H., Tebbs, S., Foltynie, T., 2017. Exenatide once weekly versus placebo in Parkinson's disease: a randomised, double-blind, placebo-controlled trial. The Lancet 6736, 31585 31584.
Bardutzky, J., Shen, Q., Henninger, N., Bouley, J., Duong, T.Q., Fisher, M., 2005. Differences in ischemic lesion evolution in different rat strains using diffusion and perfusion imaging. Stroke 36, 2000–2005.
Bederson, J.B., Pitts, L.H., Tsuji, M., Nishimura, M.C., Davis, R.L., Bartkowski, H., 1986. Rat middle cerebral artery occlusion: evaluation of the model and development of a neurologic examination. Stroke 17, 472–476.
Bomfim, T.R., Forny-Germano, L., Sathler, L.B., Brito-Moreira, J., Houzel, J.C., Decker, H., Silverman, M.A., Kazi, H., Melo, H.M., McClean, P.L., Holscher, C., Arnold, S.E., Talbot, K., Klein, W.L., Munoz, D.P., Ferreira, S.T., De Felice, F.G., 2012. An anti-diabetes agent protects the mouse brain from defective insulin signaling caused by Alzheimer's disease- associated Abeta oligomers. J. Clin. Investig. 122, 1339–1353.
Briyal, S., Shah, S., Gulati, A., 2014. Neuroprotective and anti-apoptotic effects of liraglutide in the rat brain following focal cerebral ischemia. Neuroscience 281, 269–281.
Brown, J.P., Couillard-Despres, S., Cooper-Kuhn, C.M., Winkler, J., Aigner, L., Kuhn, H.G., 2003. Transient expression of doublecortin during adult neurogenesis. J. Comp. Neurol. 467, 1–10.
Chau, M., Deveau, T.C., Song, M., Wei, Z.Z., Gu, X., Yu, S.P., Wei, L., 2017. Transplantation of iPS cell-derived neural progenitors overexpressing SDF-1alpha increases regeneration and functional recovery after ischemic stroke. Oncotarget 8, 97537–97553.
Christensen, M., Knop, F.K., Vilsboll, T., Holst, J.J., 2011. Lixisenatide for type 2 diabetes mellitus. Expert Opin. Investig. Drugs 20, 549–557.
Clark, I.A., Vissel, B., 2014. Inflammation-sleep interface in brain disease: TNF, insulin, orexin. J. Neuroinflammation 11, 51.
Couillard-Despres, S., Winner, B., Schaubeck, S., Aigner, R., Vroemen, M., Weidner, N., Bogdahn, U., Winkler, J., Kuhn, H.G., Aigner, L., 2005. Doublecortin expression levels in adult brain reflect neurogenesis. Eur. J. Neurosci. 21, 1–14.
Daniel, C., Albrecht, H., Ludke, A., Hugo, C., 2008. Nestin expression in repopulating mesangial cells promotes their proliferation. Lab. Investig. 88, 387–397.
Darsalia, V., Hua, S., Larsson, M., Mallard, C., Nathanson, D., Nystrom, T., Sjoholm, A., Johansson, M.E., Patrone, C., 2014. Exendin-4 reduces ischemic brain injury in normal and aged type 2 diabetic mice and promotes microglial M2 polarization. PLoS One 9, e103114.
Darsalia, V., Larsson, M., Lietzau, G., Nathanson, D., Nystrom, T., Klein, T., Patrone, C., 2016. Gliptin-mediated neuroprotection against stroke requires chronic pretreatment and is independent of glucagon-like peptide-1 receptor. Diabetes Obes. Metab. 18, 537–541.
Darsalia, V., Mansouri, S., Ortsater, H., Olverling, A., Nozadze, N., Kappe, C., Iverfeldt, K., Tracy, L.M., Grankvist, N., Sjoholm, A., Patrone, C., 2012. Glucagon-like peptide-1 receptor activation reduces ischaemic brain damage following stroke in Type 2 diabetic rats. Clin. Sci. (Lond.) 122, 473–483.
Dhillon, S., 2018. Semaglutide: first global approval. Drugs 78, 275–284.
Duggal, N., Schmidt-Kastner, R., Hakim, A.M., 1997. Nestin expression in reactive astrocytes following focal cerebral ischemia in rats. Brain Res. 768, 1–9.
Fan, Q.Y., Liu, J.J., Zhang, G.L., Wu, H.Q., Zhang, R., Zhan, S.Q., Liu, N., 2018. Inhibition of SNK-SPAR signaling pathway promotes the restoration of motor function in a rat model of ischemic stroke. J. Cell. Biochem. 119, 1093–1110.
Feeney, D.M., Gonzalez, A., Law, W.A., 1982. Amphetamine, haloperidol, and experience interact to affect rate of recovery after motor cortex injury. Science 217, 855–857.
Feng, P., Zhang, X., Li, D., Ji, C., Yuan, Z., Wang, R., Xue, G., Li, G., Holscher, C., 2018. Two novel dual GLP-1/GIP receptor agonists are neuroprotective in the MPTP mouse model of Parkinson's disease. Neuropharmacology 133, 385–394.
Gould, E., McEwen, B.S., Tanapat, P., Galea, L.A., Fuchs, E., 1997. Neurogenesis in the dentate gyrus of the adult tree shrew is regulated by psychosocial stress and NMDA receptor activation. J. Neurosci. 17, 2492–2498.
Greenberg, D.A., Jin, K., 2006. Neurodegeneration and neurogenesis: focus on Alzheimer's disease. Curr. Alzheimer Res. 3, 25–28.
Hamilton, A., Holscher, C., 2009. Receptors for the incretin glucagon-like peptide-1 are expressed on neurons in the central nervous system. Neuroreport 20, 1161–1166.
Han, L., Holscher, C., Xue, G.F., Li, G., Li, D., 2016. A novel dual-glucagon-like peptide-1 and glucose-dependent insulinotropic polypeptide receptor agonist is neuroprotective in transient focal cerebral ischemia in the rat. Neuroreport 27, 23–32.
Hedrington, M.S., Tsiskarishvili, A., Davis, S.N., 2018. Subcutaneous semaglutide (NN9535) for the treatment of type 2 diabetes. Expert Opin. Biol. Ther. 18, 343–351.
Holscher, C., 2014a. Central effects of GLP-1: new opportunities for treatments of neurodegenerative diseases. J. Endocrinol. 221, T31–T41.
Holscher, C., 2014b. Insulin, incretins and other growth factors as potential novel treatments for Alzheimer's and Parkinson's diseases. Biochem. Soc. Trans. 42, 593–599.
Holscher, C., 2018. Novel dual GLP-1/GIP receptor agonists show neuroprotective effects in Alzheimer's and Parkinson's disease models. Neuropharmacology 136, 251–259.
Hölscher, C., 2019. Insulin signalling impairment in the brain as a risk factor in Alzheimer's Disease. Front. Aging Neurosci. 11, 1–11.
Hunter, A.J., Hatcher, J., Virley, D., Nelson, P., Irving, E., Hadingham, S.J., Parsons, A.A., 2000. Functional assessments in mice and rats after focal stroke. Neuropharmacology 39, 806–816.
Hunter, K., Holscher, C., 2012. Drugs developed to treat diabetes, liraglutide and lixisenatide, cross the blood brain barrier and enhance neurogenesis. BMC Neurosci. 13, 33.
Jalewa, J., Sharma, M.K., Gengler, S., Holscher, C., 2017. A novel GLP-1/GIP dual receptor agonist protects from 6-OHDA lesion in a rat model of Parkinson's disease. Neuropharmacology 117, 238–248.
Kastin, A.J., Akerstrom, V., Pan, W., 2002. Interactions of glucagon-like peptide-1 (GLP-1) with the blood-brain barrier. J. Mol. Neurosci. 18, 7–14.
Kempermann, G., Song, H., Gage, F.H., 2015. Neurogenesis in the adult Hippocampus. Cold Spring Harb. Perspect. Biol. 7, a018812.
Kuhn, H.G., Dickinson-Anson, H., Gage, F.H., 1996. Neurogenesis in the dentate gyrus of the adult rat: age-related decrease of neuronal progenitor proliferation. J. Neurosci. 16, 2027–2033.
Lau, J., Bloch, P., Schaffer, L., Pettersson, I., Spetzler, J., Kofoed, J., Madsen, K., Knudsen, L.B., McGuire, J., Steensgaard, D.B., Strauss, H.M., Gram, D.X., Knudsen, S.M., Nielsen, F.S., Thygesen, P., Reedtz-Runge, S., Kruse, T., 2015. Discovery of the once-weekly glucagon-like peptide-1 (GLP-1) analogue semaglutide. J. Med. Chem. 58, 7370–7380.
Lee, C.H., Yan, B., Yoo, K.Y., Choi, J.H., Kwon, S.H., Her, S., Sohn, Y., Hwang, I.K., Cho,

J.H., Kim, Y.M., Won, M.H., 2011. Ischemia-induced changes in glucagon-like peptide-1 receptor and neuroprotective effect of its agonist, exendin-4, in experimental transient cerebral ischemia. J. Neurosci. Res. 89, 1103–1113.
Lee, Y.J., Han, S.B., Nam, S.Y., Oh, K.W., Hong, J.T., 2010. Inflammation and Alzheimer's disease. Arch Pharm. Res. (Seoul) 33, 1539–1556.
Li, Y., Perry, T., Kindy, M.S., Harvey, B.K., Tweedie, D., Holloway, H.W., Powers, K., Shen, H., Egan, J.M., Sambamurti, K., Brossi, A., Lahiri, D.K., Mattson, M.P., Hoffer, B.J., Wang, Y., Greig, N.H., 2009. GLP-1 receptor stimulation preserves primary cortical and dopaminergic neurons in cellular and rodent models of stroke and Parkinsonism. Proc. Natl. Acad. Sci. U. S. A. 106, 1285–1290.
Liu, W., Jalewa, J., Sharma, M., Li, G., Li, L., Holscher, C., 2015. Neuroprotective effects of lixisenatide and liraglutide in the 1-methyl-4-phenyl-1,2,3,6-tetrahydropyridine mouse model of Parkinson's disease. Neuroscience 303, 42–50.
Longa, E.Z., Weinstein, P.R., Carlson, S., Cummins, R., 1989. Reversible middle cerebral artery occlusion without craniectomy in rats. Stroke 20, 84–91.
Lovshin, J.A., Drucker, D.J., 2009. Incretin-based therapies for type 2 diabetes mellitus. Nat. Rev. Endocrinol. 5, 262–269.
Malek, R., Borowicz, K.K., Jargiello, M., Czuczwar, S.J., 2007. Role of nuclear factor kappaB in the central nervous system. Pharmacol. Rep. 59, 25–33.
Marini, C., Baldassarre, M., Russo, T., De Santis, F., Sacco, S., Ciancarelli, I., Carolei, A., 2004. Burden of first-ever ischemic stroke in the oldest old: evidence from a population-based study. Neurology 62, 77–81.
Marso, S.P., Bain, S.C., Consoli, A., Eliaschewitz, F.G., Jodar, E., Leiter, L.A., Lingvay, I., Rosenstock, J., Seufert, J., Warren, M.L., Woo, V., Hansen, O., Holst, A.G., Pettersson, J., Vilsboll, T., Investigators, S., 2016a. Semaglutide and cardiovascular outcomes in patients with type 2 diabetes. N. Engl. J. Med. 375, 1834–1844.
Marso, S.P., Daniels, G.H., Brown-Frandsen, K., Kristensen, P., Mann, J.F., Nauck, M.A., Nissen, S.E., Pocock, S., Poulter, N.R., Ravn, L.S., Steinberg, W.M., Stockner, M., Zinman, B., Bergenstal, R.M., Buse, J.B., Committee, L.S., Investigators, L.T., 2016b. Liraglutide and cardiovascular outcomes in type 2 diabetes. N. Engl. J. Med. 375, 311–322.
McClean, P.L., Holscher, C., 2014. Liraglutide can reverse memory impairment, synaptic loss and reduce plaque load in aged APP/PS1 mice, a model of Alzheimer's disease. Neuropharmacology 76 (Pt A), 57–67.
Meyer, G., Perez-Garcia, C.G., Gleeson, J.G., 2002. Selective expression of doublecortin and LIS1 in developing human cortex suggests unique modes of neuronal movement. Cerebr. Cortex 12, 1225–1236.
Muir, K.W., Tyrrell, P., Sattar, N., Warburton, E., 2007. Inflammation and ischaemic stroke. Curr. Opin. Neurol. 20, 334–342.
Neth, B.J., Craft, S., 2017. Insulin resistance and alzheimer's disease: bioenergetic linkages. Front. Aging Neurosci. 9, 345.
Nito, C., Kamiya, T., Ueda, M., Arii, T., Katayama, Y., 2004. Mild hypothermia enhances the neuroprotective effects of FK506 and expands its therapeutic window following transient focal ischemia in rats. Brain Res. 1008, 179–185.
Ohlsson, A.L., Johansson, B.B., 1995. Environment influences functional outcome of cerebral infarction in rats. Stroke 26, 644–649.
Parthsarathy, V., Holscher, C., 2013. Chronic treatment with the GLP1 analogue liraglutide increases cell proliferation and differentiation into neurons in an AD mouse model. PLoS One 8, e58784.
Pin-Barre, C., Laurin, J., Felix, M.S., Pertici, V., Kober, F., Marqueste, T., Matarazzo, V., Muscatelli-Bossy, F., Temprado, J.J., Brisswalter, J., Decherchi, P., 2014. Acute neuromuscular adaptation at the spinal level following middle cerebral artery occlusion-reperfusion in the rat. PLoS One 9, e89953.
Qiao, H., Zhang, X., Zhu, C., Dong, L., Wang, L., Zhang, X., Xing, Y., Wang, C., Ji, Y., Cao, X., 2012. Luteolin downregulates TLR4, TLR5, NF-kappaB and p-p38MAPK expression, upregulates the p-ERK expression, and protects rat brains against focal ischemia. Brain Res. 1448, 71–81.
Sato, K., Kameda, M., Yasuhara, T., Agari, T., Baba, T., Wang, F., Shinko, A., Wakamori, T., Toyoshima, A., Takeuchi, H., Sasaki, T., Sasada, S., Kondo, A., Borlongan, C.V., Matsumae, M., Date, I., 2013. Neuroprotective effects of liraglutide for stroke model of rats. Int. J. Mol. Sci. 14, 21513–21524.
Sharma, M.K., Jalewa, J., Holscher, C., 2014. Neuroprotective and anti-apoptotic effects of liraglutide on SH-SY5Y cells exposed to methylglyoxal stress. J. Neurochem. 128, 459–471.
Sunabori, T., Tokunaga, A., Nagai, T., Sawamoto, K., Okabe, M., Miyawaki, A., Matsuzaki, Y., Miyata, T., Okano, H., 2008. Cell-cycle-specific nestin expression coordinates with morphological changes in embryonic cortical neural progenitors. J. Cell Sci. 121, 1204–1212.
Takamori, Y., Mori, T., Wakabayashi, T., Nagasaka, Y., Matsuzaki, T., Yamada, H., 2009. Nestin-positive microglia in adult rat cerebral cortex. Brain Res. 1270, 10–18.
Talbot, K., Wang, H.Y., 2014. The nature, significance, and glucagon-like peptide-1 analog treatment of brain insulin resistance in Alzheimer's disease. Alzheimers Dementia 10, S12–S25.
Teramoto, S., Miyamoto, N., Yatomi, K., Tanaka, Y., Oishi, H., Arai, H., Hattori, N., Urabe, T., 2011. Exendin-4, a glucagon-like peptide-1 receptor agonist, provides neuroprotection in mice transient focal cerebral ischemia. J. Cereb. Blood Flow Metab. 31, 1696–1705.
Wang, C., Lv, H., Li, Q., Gong, K., Yang, L.L., Wei, Z., Pan, Y., Wang, M., 2019. RNA sequencing of peripheral blood revealed that the neurotropic TRK receptor signaling pathway shows apparent correlation in recovery following spinal cord injury at small cohort. J. Mol. Neurosci. 35 (4), 724–734.
Yin, X.M., Oltvai, Z.N., Korsmeyer, S.J., 1995. Heterodimerization with Bax is required for Bcl-2 to repress cell death. Curr. Top. Microbiol. Immunol. 194, 331–338.
Zhang, L., Zhang, L., Li, L., Holscher, C., 2018. Neuroprotective effects of the novel GLP-1 long acting analogue semaglutide in the MPTP Parkinson's disease mouse model. Neuropeptides 71, 70–80.
Zhang, L., Zhang, L., Li, L., Holscher, C., 2019. Semaglutide is neuroprotective and reduces alpha-synuclein levels in the chronic MPTP mouse model of Parkinson's disease. J. Parkinson's Dis. 9, 157–171.
Zhang, R.L., Zhang, Z.G., Chopp, M., 2008. Ischemic stroke and neurogenesis in the subventricular zone. Neuropharmacology 55, 345–352.